Chen, K. and Khalighi, B., "A CFD Study of Drag Reduction Devices for a Full Size Production Pickup Truck," SAE Technical Paper 2015-01-1541, 2015, doi:10.4271/2015-01-1541.

Conference Paper · April 2015

DOI: 10.4271/2015-01-1541

Kuo-Huey Chen
General Motors Company

SAE INTERNATIONAL®

A CFD Study of Drag Reduction Devices for a Full Size Production Pickup Truck

2015-01-1541
Published 04/14/2015

Kuo-Huey Chen and Bahram Khalighi
General Motors Global R&D

CITATION: Chen, K. and Khalighi, B., "A CFD Study of Drag Reduction Devices for a Full Size Production Pickup Truck," SAE Technical Paper 2015-01-1541, 2015, doi:10.4271/2015-01-1541.

Abstract

Various drag reduction strategies have been applied to a full size production pickup truck to evaluate their effectiveness by using Computational Fluid Dynamics (CFD). The drag reduction devices evaluated in this study were placed at the rear end of the truck bed and the tailgate. Three types of devices were evaluated: (1) boat tail-like extended plates attached to the tailgate; (2) mid-plate attached to the mid-section of the tailgate and; (3) flat plates partially covering the truck bed. The effect of drag reduction by various combinations of these three devices are presented in this paper. Twenty-four configurations were evaluated in the study with the best achievable drag reduction of around 21 counts ($\Delta Cd = 0.021$). A detailed breakdown of the pressure differentials at the base of the truck is provided in order to understand the flow mechanism for the drag reductions. It is concluded that the added surfaces near the tailgate lower the static pressure on the inner side of the tailgate in addition to the pressure increase at the base (outer side of the tailgate).

Introduction

For most road vehicles, improvements to the wake flow characteristics offer the largest payoff for drag reduction. The main contributions to aerodynamic drag arise from separated flows in the rear, causing pressure recovery losses, and the creation of vorticity in the wake [1, 2, 3, 4, 5, 6]. The near wake is a fluctuating flow field which makes the aerodynamic drag highly unsteady, although only the time averaged drag force is usually of practical interest. Initial efforts to reduce drag of the ground vehicle bodies concentrated mainly on making changes to the areas with attached flows [1, 2]. Research in the last few decades motivated in part by increased fuel cost and emissions have led to significant advances in understanding of drag reduction mechanisms for blunt-based bluff bodies. An overview of techniques proposed for drag reduction for bluff bodies is given by [7]. Some of these techniques include plates installed on the base of the vehicles [8, 9, 10], base bleed [11] and trailing edge modifications [3], and reducing aerodynamic drag by stabilizing the large-scale vortical motions in the near wake. The effectiveness of these techniques depends on the nature of the large-scale flow motions in the wake as well as the receptivity and amplification of disturbances in the separated shear layers. One method of altering the pressure distributions is to add four extension plates to the base of a square-back (SB) model to prevent or modify unsteady vortex formation [8, 12].

The pickup truck segment is now accounting for a large percentage of the total annual light vehicle sales in the U.S. This development in the marketplace suggests that the pickup trucks will have an increasingly larger weighting in the national oil consumption and automakers' CAFÉ (corporate average fuel economy) calculations. Thus aerodynamic performances of pickup trucks will become increasingly more important for the automakers, and for the society at large. Recent studies in aerodynamic drag and flow field for pickup trucks including measurements [13] for a reduced scale pickup truck and numerical investigations [14, 15]. The aerodynamics of pickup trucks is more complex than other open bed trucks or SUV because the short length of the bed can result in interaction of the bed walls and tailgate with the separated shear layer formed at the edge of the cab.

The present study focuses on implementing some drag reduction devices, similar to the techniques used for a square-back geometry (SB) by [12]. The production vehicle topology of pickup truck with rough underbody and a huge open truck bed space is very different from the SB model. The effectiveness of such similar drag reduction devices applied to the pickup truck remains to be understood. The drag reduction devices are plates appended to the rear end of the pickup truck around the tail gate.

The structure of the paper is as follows: The baseline truck and the modified truck models with drag reduction devices are defined first. Next, the CFD analysis approach and numerical setup used in this study are described. The drag reduction predictions for twenty-four configurations are presented and compared with the baseline. Finally, discussions and conclusions are drawn by looking into the pressure, flow field and Cd breakdown on the major contributing surfaces for some of the cases.

Full Size Production Pickup Truck

The Baseline Truck Model

The baseline full size pickup truck model is shown in Fig. 1. The pertinent dimensions are: 5.8 m × 2.0 m × 1.8 m in x, y, z directions, respectively. The figure shows the top, side, bottom, front and the rear views of the pickup truck. The model is a close representation of the production version with detailed underhood and underbody components.

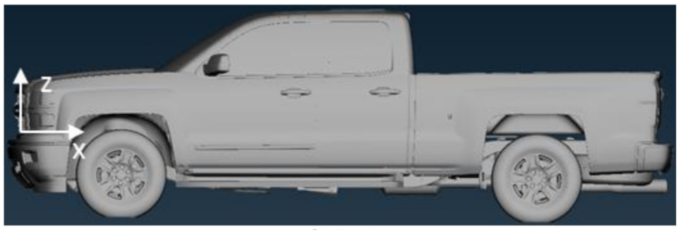

(a) Side view

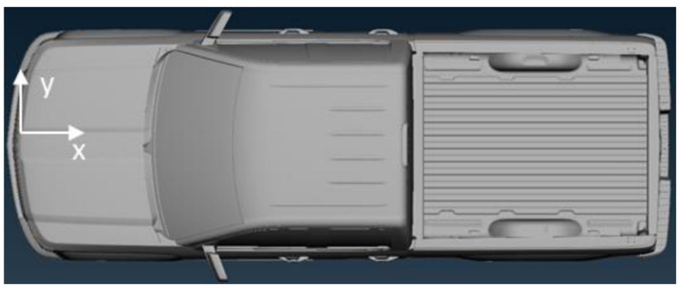

(b) Top view

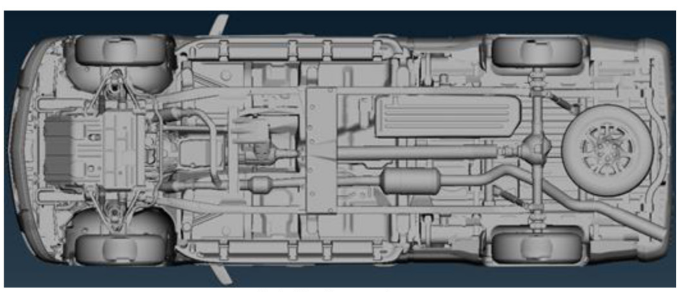

(c) Bottom view

(d) Front view

(e) Rear view

Figure 1. The baseline pickup truck model: (a) side view; (b) top view; (c) bottom view; (d) front view; (e) rear view.

The Drag Reduction Devices

Three types of plates are attached to the tailgate for this study: (1) boat tail-like plates with taper, (2) mid plate and (3) partial truck bed cover plate. The dimensions of the plates considered in the study are limited to the size of the tail gate for practical and feasible implementations.

Boat Tail Plates

Inspired by the square back model for drag reduction study [12], boat tail-like extended plates were attached to the tailgate of the truck. Figure 2 shows the modified model with extended plates and the relevant dimensions. With combinations of the plates, one can form a "boat tail box" attached to the tailgate. As shown in Fig. 2, there is a 9 degree taper angle on four sides of the box toward the rear end. This angle was based on our previous study for the square back model [12] and was not optimized for the truck in this study. In the lengthwise of the box, it was further divided into two so that half-length box could also be studied. The rear end of the box can be removed so that a hollow box (cavity) can be studied. Small winglets on top of the box were also added to study their effect on the drag reduction. In our CFD study, all surfaces are baffle-like plates with zero thickness so that they can be added or removed computationally to create many configurations and evaluate the drag quickly and more consistently in a single mesh setting.

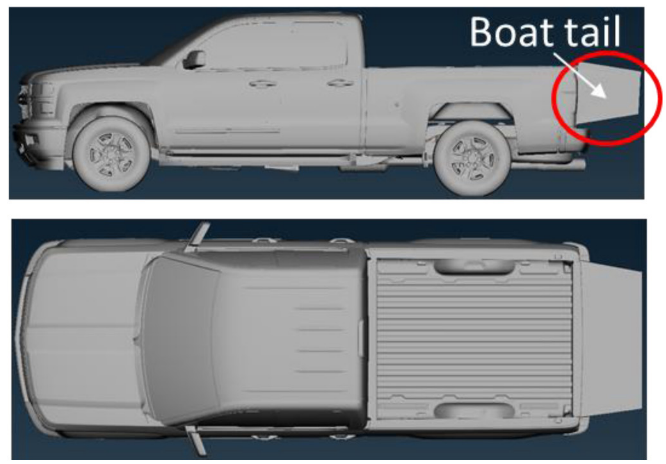

(a). Boat tail plates attached to the tailgate: (top) side view and (bottom) top view.

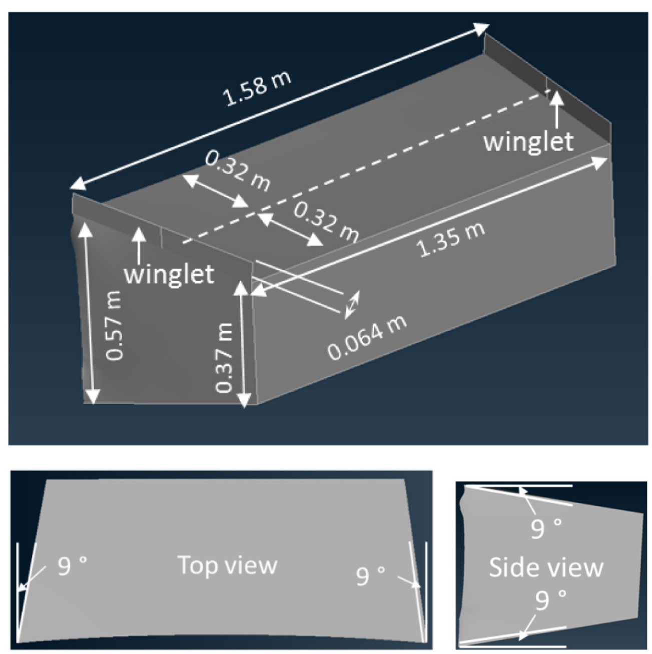

(b). Boat tail plate dimensions.

Figure 2. The modified truck model: (a) with boat tail plates attached to the tailgate, (b) the dimensions.

Mid Plate

A "mid plate" was attached to the tailgate at about mid-section of the tailgate height as shown in Fig. 3. The length of the mid plate (0.32 m) is about half of the tailgate height so that it can be conveniently folded (or installed by other means) as part of the lower half of the tailgate and deployed.

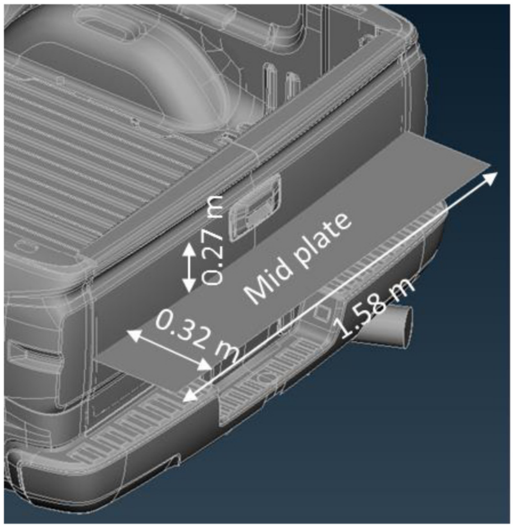

Figure 3. The modified truck model with mid-plate attached to the middle of the tailgate.

Partial Truck Bed Cover

Figure 4 shows a plate which partially covers the truck bed. Two different cover lengths were investigated, namely Partial bed cover 1 with a length of 0.64 m and Partial bed cover 2 with 0.32 m. The size of the plate is again limited to the tailgate height (0.64 m) so that it can be practically stowed and hidden inside the tailgate and deployed when needed.

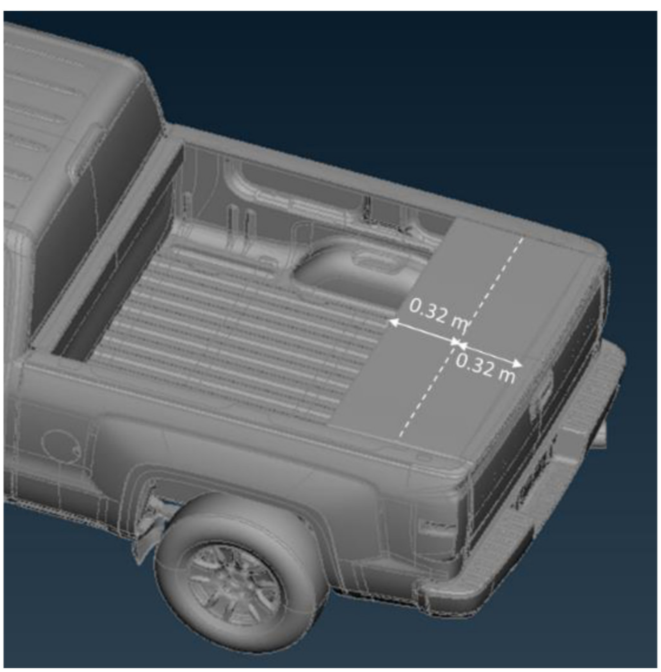

Figure 4. Partial truck bed cover and dimensions.

Numerical Setup

Figure 5 shows the model and its location in a virtual wind tunnel. The dimensions of the test section are 21.3 m (length) × 10.4 m (width) × 5.4 m (height). The front of the vehicle is at a distance about 67% of the vehicle length from the inlet. Both the tunnel floor and the four tires are held stationary. The inlet velocity is 30.56 m/s with 0.6% turbulent intensity. Constant atmosphere pressure is specified at the exit. Symmetry condition is used at the top, side and the floor planes. All the vehicle surfaces were non-slip wall condition. Total volume mesh count is 39 million for the CFD model, of which about 5 million prismatic cells (10 layers) were applied to resolve the boundary region surrounding the vehicle surfaces except the underbody and the truck bed. The surface mesh sizes vary between 2 to 10 mm depending on the local geometry resolution. The first layer of the prismatic mesh away from the vehicle surface is about 1 mm. Far away from the model, the mesh size on the tunnel walls is 200 mm. Figure 6 shows mesh layouts in two cutting planes: one in the mid tunnel plane from inlet to exit and the other from side to side of the tunnel cutting through the roof of the cabin. Fluent version 15.0 [16] was used for the simulation. Steady state Reynolds averaged equations were solved. Second order upwind spatial discretization were used for all calculations. SIMPLE scheme was used to treat the pressure-velocity coupling. A Realizable k-epsilon turbulence model with non-equilibrium wall functions was used for the closure of the turbulence equations.

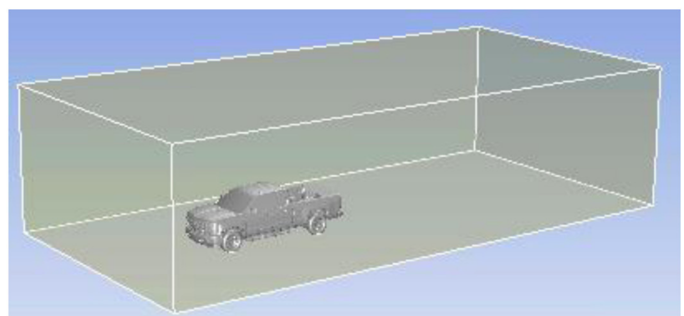

Figure 5. The pickup truck model in the virtual wind tunnel.

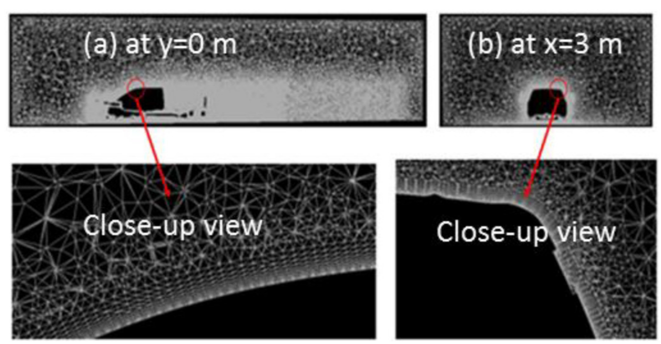

Figure 6. Mesh layouts on two cutting planes: (a) y=0; (b) x= 3 m with close-up details.

Results And Discussions

Flow Configurations

Table 1 summarizes the various drag reduction devices attached to the rear end of the truck bed and the tailgate (24 CFD cases). The original truck is defined as the baseline which is also designated as

Case 1. Cases 2 to 24 are clearly defined in the table. Only one CFD volume mesh was used for all twenty-four cases. This was achieved by turning one or more plates from wall condition to interior zone and vice versa in order to create different cases. By doing so, drag evaluation was done consistently for all cases in a single mesh environment.

Drag Evaluation

Drag convergence history is shown in Fig. 7. Due to the nature of the bluff body-like geometry of the truck, Cd values toward the end of the simulation exhibit a dynamically stable pattern. To evaluate drags for direct comparisons, the averaged values at the final 1000, 2000 and 3000 iterations are calculated, respectively.

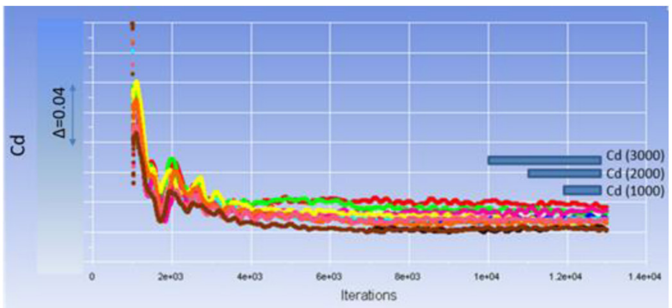

Figure 7. Cd convergence history for cases.

Table 2 summarizes the drag coefficient differentials ΔCd compared to the baseline for all cases. As shown in the table, the difference between three drag averages for all cases is less than one count so that the dynamically stable values are practically achieved for all simulations. Compared to the baseline (Case 1), not all devices contribute favorably to the drag reduction. As shown in Table 2, Cases 2, 3, 6 and 20 have higher Cd values than the baseline. Cases 2 and 3 indicate that the bottom plates alone have negative impact on the drag. Also half side plate in Case 6 shows a negative contribution for drag reduction. However, using full length of the side plates in Case 15 shows about 2 count reduction in Cd. The mid-plate alone in Case 20 increases Cd almost five counts. From the results shown in Table 2, the drag reduction effectiveness can be categorized in three groups:

1. About 5 counts Cd reduction associated with half-length top plate implementation.
2. About 10 counts Cd reduction with full-length top plate implementation.
3. About 14 to 21 counts Cd reduction with the combination of the partial truck bed cover (Partial bed cover 1 or Partial bed cover 2) and the top plate implementation.

It was observed that the main contributors for the Cd reduction are from the top plate and the partial truck bed cover. Any combination associated with these two devices can produce favorable drag reduction. For cases 10, 11, 12, 13, 14, 16 and 17, where full-length top plate was used, the Cd reductions were about 10 counts. However, the reduction was about 5 counts if only the half-length was used (Case 7, 8 and 9). It also shows that the partial truck bed cover alone can have a significant impact on the drag reduction. It reveals that the Partial bed cover 2 implementation in Case 21 reduces 10 counts and the Partial bed cover 1 used in Case 19 achieves 16 counts Cd reduction.

Combination of both partial truck bed cover and the top plate are the most promising devices for drag reduction. The extent of the Cd reduction depends on the length of the plates. As shown in Cases 22, 23 and 24, the best achievable Cd of 21 count reduction is in Case 23 where full length was used for both plates. With both plates in half-length shown in Case 24, the Cd reduction is 14 counts.

Flow Fields and Pressure Contours

For vehicle aerodynamics, drag is mainly due to the pressure differential between the front and the rear end of the vehicle. This contributes to more than 70% of the total drag and the rest is from the viscous drag. In order to understand the effect of the added devices in reducing drag, we will examine the flow field and the local pressure distributions. Figure 8 shows the velocity vectors on the mid-plane (y=0 m) for three cases: Case 1 (baseline), Case 19 and Case 23. For the baseline, the main recirculation bubble originates from the cabin roof, covers the entire truck bed and stops at the vertical wall of the tail gate. With added partial truck bed cover (Cases 19 and 23), in addition to one main clockwise recirculation bubble inside the truck bed for the baseline, there is another weaker counter-clockwise recirculation bubble in Cases 19 and 23. The size of the main clockwise recirculation bubbles in Cases 19 and 23 are smaller than the baseline because the main recirculation bubble has to terminate at the front edge of the truck's partial bed cover. Also, the overall wake behind the tailgate for Cases 19 and 23 is taller than the baseline due to the partial truck bed cover and/or top plate (see Fig. 9 and also Fig.10). The center of the vortex in the wake region shifts toward downstream compared to the baseline.

The pressure contours in Fig. 9 (b) shows the pressures for Cases 19 and 23 on the outer-side of the tailgate (facing the wake) are higher than the baseline and the pressure on the inner-side (facing the truck bed) is lower than the baseline. This pressure differential on the tailgate improves the drag reduction. Figure 10 shows a close-up view of the velocity contours for Case 1 and 17 (with top plate only). Also it should be noted that the high number of velocity vectors just behind the tailgate in Fig. 8 is due to the mesh resolution in order to resolve the walls in the boat tail box; however, most of them are turned to interior zones (non-wall) for these three cases. Indeed, the velocity contours in Fig. 9 show smooth display despite of the mesh clustering in the boat tail region.

Table 1. Twenty-four Drag reduction configurations used in the study.

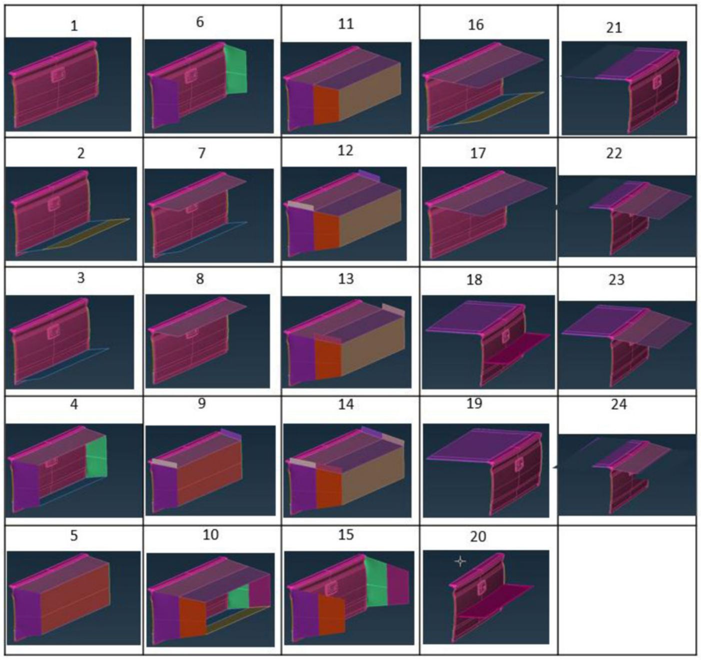

	Configuration		
1	Baseline	13	Full-length closed box with 2nd wings
2	Full-length bottom plate only	14	Full-length closed box with all wings
3	Half-length bottom plate only	15	Full-length side plates
4	Half-length open box	16	Full-length top & bottom plates
5	Half-length closed box	17	Full-length top plate only
6	Half-length side plates only	18	Partial bed cover 1 with mid-plate
7	Half-length top & bottom plates	19	Partial bed cover 1 only
8	Half-length top plate only	20	Mid-plate only
9	Half-length closed box with wings	21	Partial bed cover 2 only
10	Full-length open box	22	Partial bed cover 2 with full-length top plate
11	Full-length closed box	23	Partial bed cover 1 with full-length top plate
12	Full-length closed box with 1st wings	24	Partial bed cover 2 with half-length top plate

Table 2. Delta Cd comparisons to baseline case.

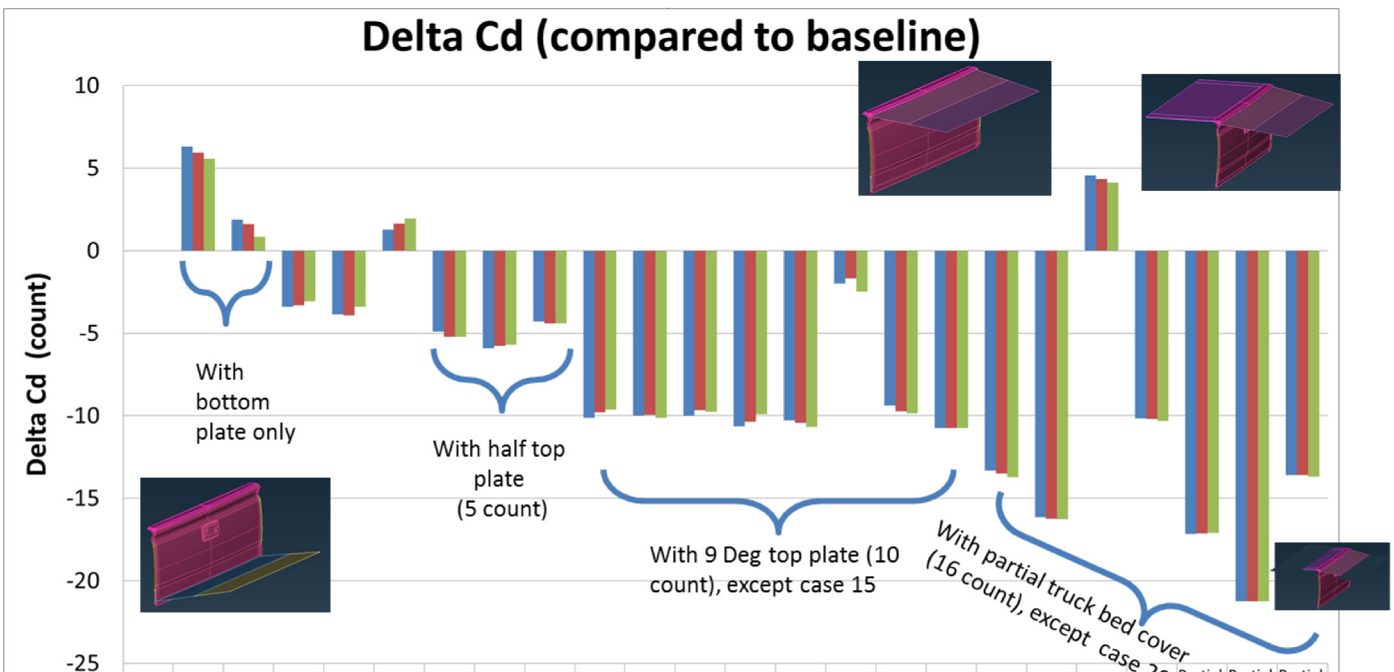

Case No.:	1	2	3	4	5	6	7	8	9	10	11	12
	Baseline	Full-length bottom plate only	Half-length bottom plate only	Half-length open box	Half-length closed box	Half-length side plates only	Half-length top & bottom plates	Half-length top plate only	Half-length closed box with wings	Full-length open box	Full-length closed box	Full-length closed box with 1st wings
Cd Δ (3000)	0.0	6.3	1.9	-3.4	-3.9	1.3	-4.9	-5.9	-4.3	-10.1	-10.0	-10.0
Cd Δ (2000)	0.0	5.9	1.6	-3.3	-3.9	1.6	-5.2	-5.8	-4.4	-9.8	-10.0	-9.7
Cd Δ (1000)	0.0	5.6	0.8	-3.1	-3.4	1.9	-5.2	-5.7	-4.4	-9.6	-10.1	-9.7

Case No.:	13	14	15	16	17	18	19	20	21	22	23	24
	Full-length closed box with 2nd wings	Full-length closed box with all wings	Full-length side plates	Full-length top & bottom plates	Full-length top plate only	Partial bed cover 1 with mid-plate	Partial bed cover 1 only	Mid-plate only	Partial bed cover 2 only	Partial bed cover 2 with full-length top plate	Partial bed cover 1 with full-length top plate	Partial bed cover 2 with half-length top plate
Cd Δ (3000)	-10.6	-10.3	-2.0	-9.4	-10.7	-13.3	-16.1	4.6	-10.2	-17.2	-21.2	-13.6
Cd Δ (2000)	-10.4	-10.4	-1.7	-9.7	-10.8	-13.5	-16.2	4.3	-10.2	-17.1	-21.2	-13.6
Cd Δ (1000)	-9.9	-10.7	-2.5	-9.8	-10.8	-13.7	-16.3	4.1	-10.3	-17.1	-21.2	-13.7

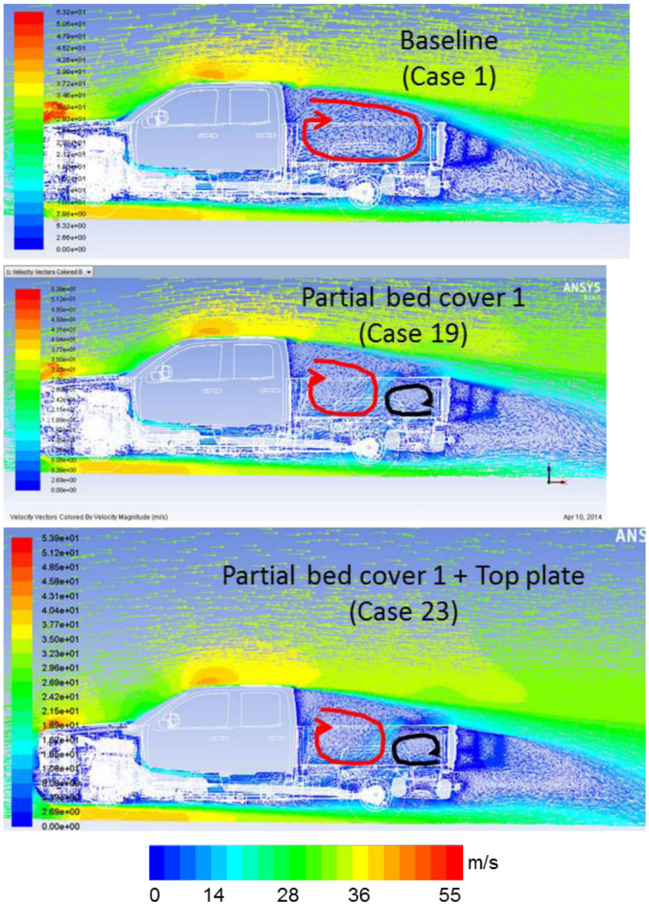

Figure 8. Velocity vectors along the mid-plane for baseline (Case 1), Partial bed cover 1 only (Case 19) and Partial bed cover 1 with top plate (Case 23).

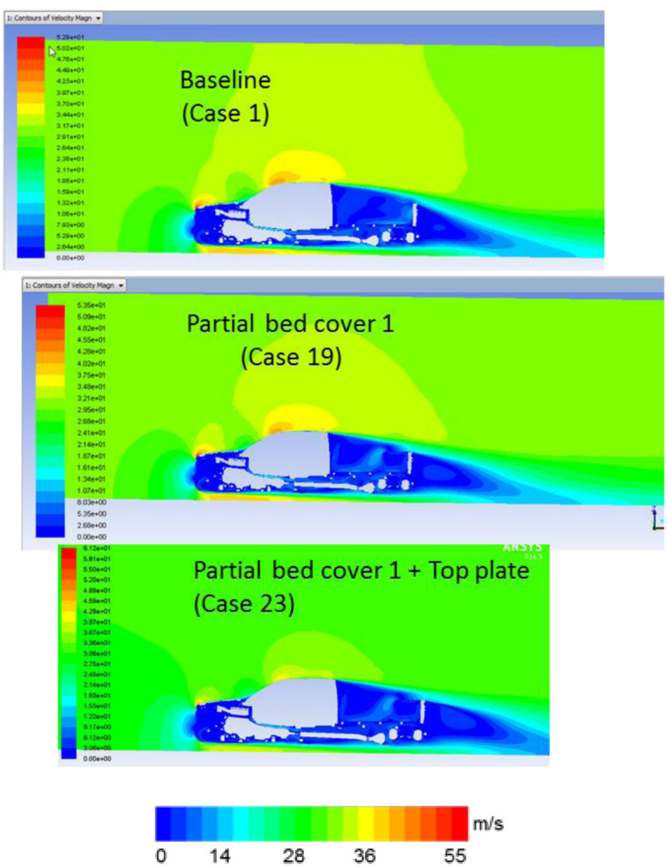

(a). Velocity contours

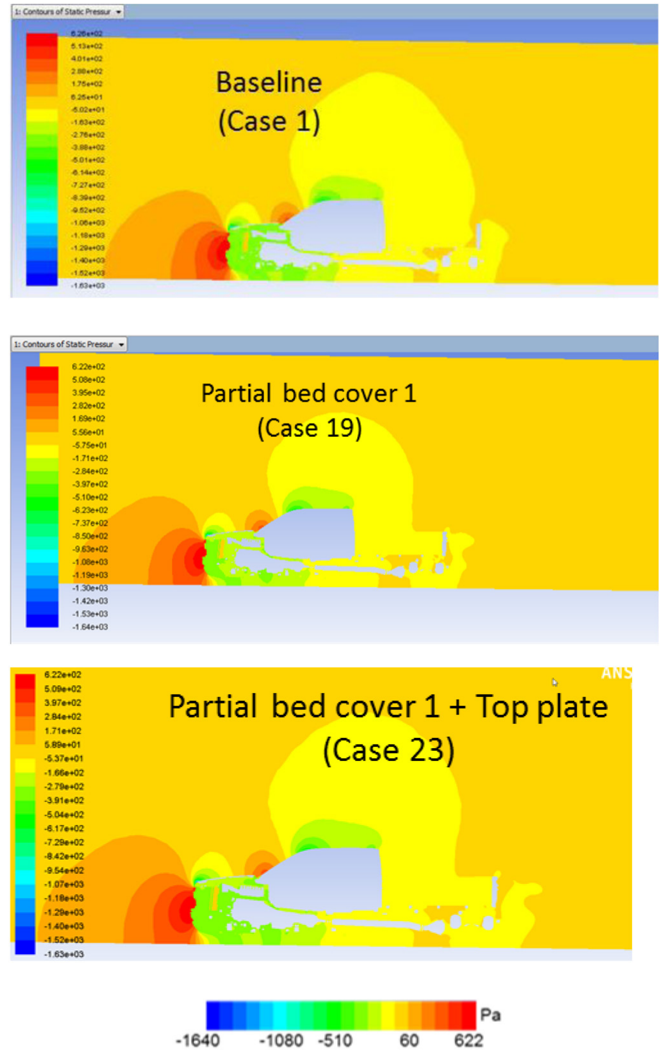

(b). Pressure contours

Figure 9. (a) Velocity; (b) pressure contours along the mid-plane for baseline (Case 1), Partial bed cover 1 only (Case 19) and Partial bed cover 1 with top plate (Case 23).

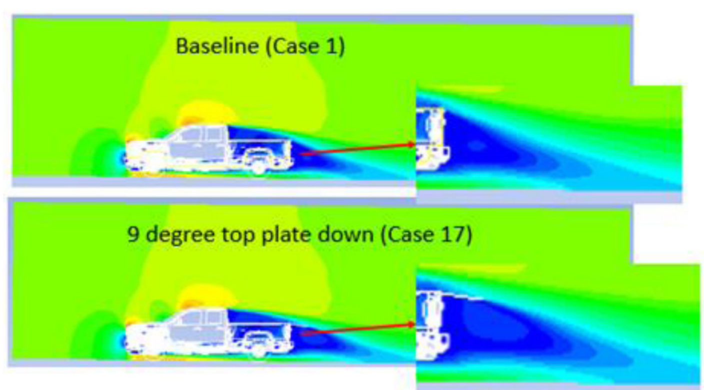

(a). Velocity contours at y= 0 plane.

Figure 10. Velocity contours for Case 1 (baseline) and Case 17 (top plate only): (a) at y=0 plane; (b) at z=1 m plane.

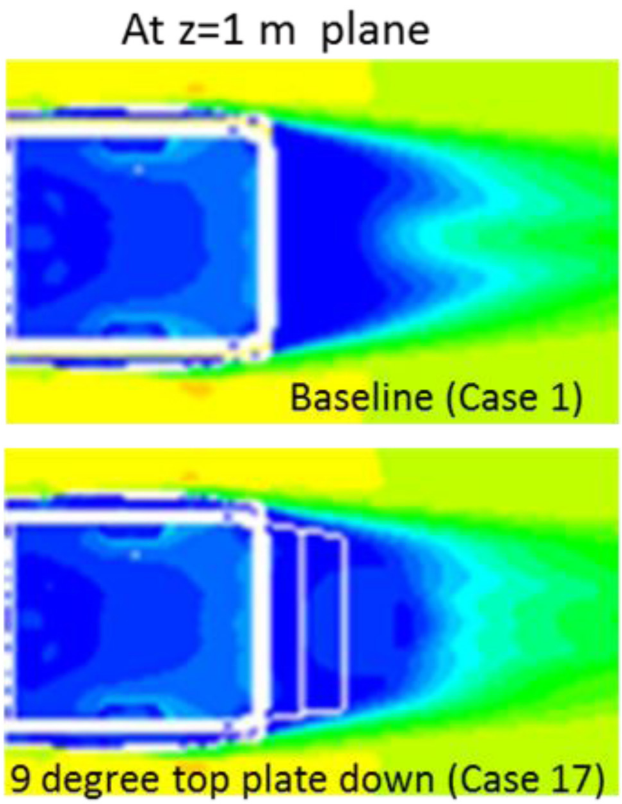

(b). Velocity contours at z=1 m plane.

Figure 10 (cont). Velocity contours for Case 1 (baseline) and Case 17 (top plate only): (a) at y=0 plane; (b) at z=1 m plane.

Pressure Differentials and ΔCd on Three Main Drag Contributing Surfaces

Figure 9 shows the pressure contours only on the mid-plane and qualitatively indicates better base pressure recovery when the partial truck bed cover and/or top plate are used. In order to understand how the pressure redistributions affect the drag for all cases, the three main surfaces that have the most pressure differentials compared to the baseline are shown in Table 3. These three surfaces are: (1) outer-side tailgate surface, (2) inner-side tailgate surface and (3) rear cab surface. The ΔP shown in Table 3 is calculated by the following equation for each surface:

$$(\Delta P)_{\text{case-x}} = (P_{avg})_{\text{case-x}} - (P_{avg})_{\text{baseline}} \tag{1}$$

Table 3 shows ΔP comparisons for five cases, i.e. Cases 10, 19, 21, 23 and 24 are shown. The ΔPs are significantly lower than the baseline (negative values) for the inner-side tailgate surface for Cases 19, 21, 23 and 24, where the partial truck bed cover is installed. The Partial bed cover 1 has approximately twice the reduction of the ΔP values than the Bed cove 2 (−48 vs. −23 Pascal). The negative ΔP values on this surface contribute favorably toward drag reduction. Also with the extended surfaces attached to the rear end of the tailgate, the ΔPs are modestly increased for the outer-side tailgate surface for all cases shown. This also has favorable impact on the drag reduction. However, the size reduction of the clockwise recirculation bubble has negative impact on drag reduction due to lower pressure on the rear cab surface. The final pressure drag number is the integration of the static pressure acting on all surfaces.

Table 3. Average ΔP (in Pascal) on three vertical surfaces (compared to baseline case)

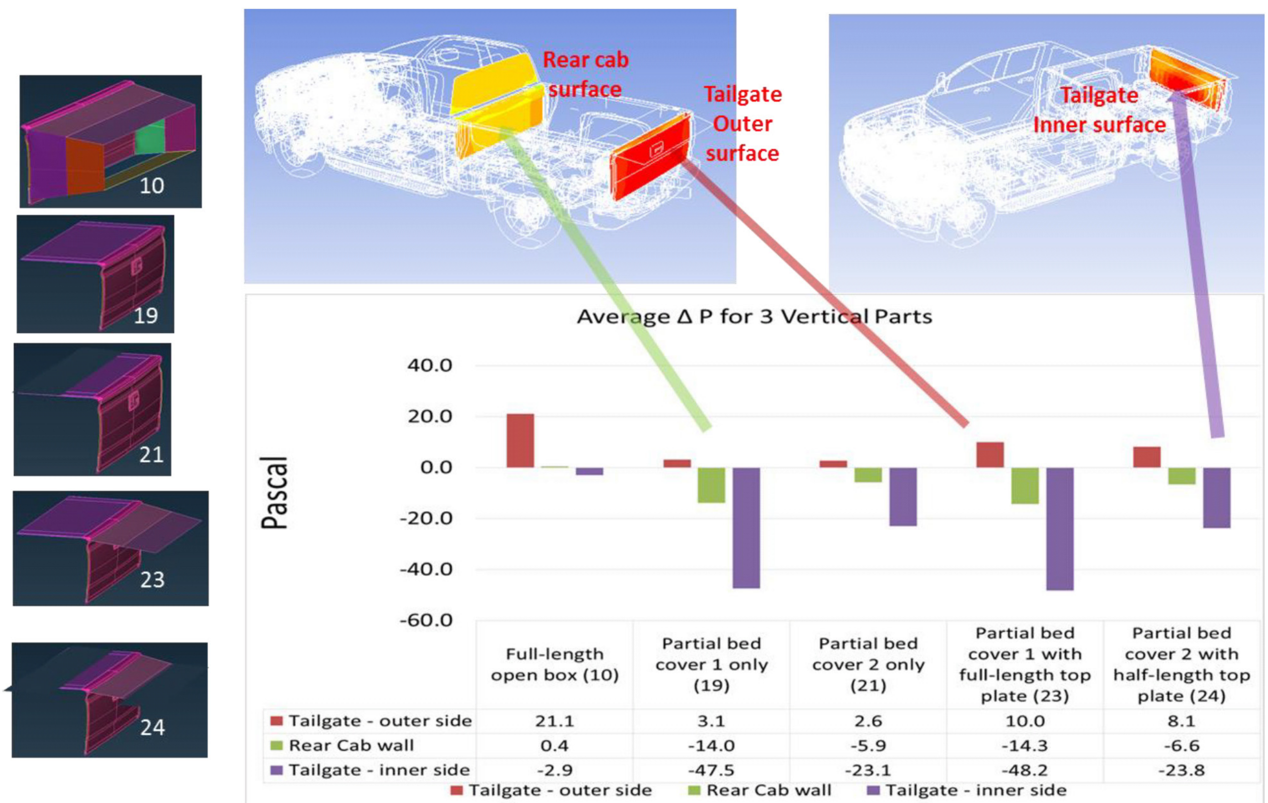

	Full-length open box (10)	Partial bed cover 1 only (19)	Partial bed cover 2 only (21)	Partial bed cover 1 with full-length top plate (23)	Partial bed cover 2 with half-length top plate (24)
Tailgate - outer side	21.1	3.1	2.6	10.0	8.1
Rear Cab wall	0.4	-14.0	-5.9	-14.3	-6.6
Tailgate - inner side	-2.9	-47.5	-23.1	-48.2	-23.8

The main Cd contributors from the vehicle surfaces are listed in Table 4. The main surfaces listed in this table are similar to those in Table 3 where the pressure differentials are presented. Four types of surfaces are listed in Table 4. They are: (1) outer-side tailgate surface, (2) inner-side tailgate surface, (3) added surfaces and (4) other surfaces. The (1) and (2) are obvious and have been explained in Table 3. The added surfaces are the drag reduction devices. Finally the other surfaces are the rear cab surface and other miscellaneous surfaces near the tailgate. Only six representative cases are listed in Table 4. They are Cases 17, 10, 19, 21, 23 and 24. A brief summary for the Cd reduction is provided as follows.

1. For the outer-side tailgate surface: In general, it has about 5.5 counts reduction if the full-length top plate is used, such as Cases 17 and 23. The open box used in Case 10 has 10 counts reduction.
2. For the inner-side tailgate surface: With the Partial bed cover 1, it achieves 26 counts reduction as seen in Cases 19 and 23. The half-length bed (Partial bed cover 2) has about 13 counts reduction as seen in Cases 21 and 24. Without the partial truck bed cover, the reduction is very minimum (Cases 10 and 17).
3. For the added surfaces: The added surface increases the Cd by less than 1 count. They are not the major players.
4. For rear cab surface: The rear cab "vertical" surface's Cd is increased by about 14 and 6 counts, respectively only for the cases with Partial bed cover 1 or Partial bed cover 2. Without the partial truck bed cover installed, the Cd change at the surface is very minimum.
5. For the total Cd reduction: The total Cd reduction for each case accounts for all surfaces of the vehicle in the simulation. This number is very close to the summation of four main Cd contributors discussed above.

Conclusions

This paper investigates drag reduction strategies applied to a full size production pickup truck using CFD. The drag reduction devices were placed at the rear end of the truck bed and the tailgate. Three types of devices were evaluated: (1) boat tail-like extended plates attached to the tailgate; (2) mid-plate attached to the mid-section of the tailgate and; (3) flat plates partially covering the truck bed. The combination of these plates generates twenty-four configurations for the Cd evaluation. Among the cases, the best achievable Cd reduction of about 21 counts (ΔCd = 0.021) was achieved by Case 23 which implements both the Partial bed cover 1 and the top plate. A detailed breakdown of the pressure differentials at the base indicates that the added surfaces near the tailgate lowers the static pressure on the inner-side tailgate surface in addition to the pressure increase on the outer-side tailgate surface.

The twenty-four cases presented in this paper obviously do not include all possible combinations. However, we believe that the benefit of using such drag reduction devices for the pickup truck can be explored with the cases included so far. Nevertheless, tunnel tests for selected promising devices such as Cases 17, 19, 23 and 24 have to be conducted in order to confirm the effectiveness of these devices.

Table 4. Main Cd (count) reduction contributors

	Tailgate Outer surface	Tailgate Inner surface	Added surfaces	Other surfaces	Total
17	-5.54	-1.25	-1.0	-1.8	ΔCd= -10.7
10	-9.9	-2.14	+0.6	+1.4	ΔCd= -10.0
19	-2.8	-26.0	+0.8	+13.7	ΔCd= -16.2
21	-2.6	-12.8	+0.4	+6.2	ΔCd= -10.2
23	-5.5	-26.4	+0.46	+13.9	ΔCd= -21.2
24	-4.7	-13.2	+0.5	+6.7	ΔCd= -13.7

References

1. Duell, E. and George, A., "Measurements in the Unsteady Near Wakes of Ground Vehicle Bodies," SAE Technical Paper 930298, 1993, doi:10.4271/930298.
2. Duell, E. G and George, A. R, 1992. "Unsteady Wake Flows of Ground Vehicle Bodies, AIAA Paper 92-2641, AIAA 10th Applied Aerodynamics Conference.
3. Han, T., 1989. Computational Analysis of Three-Dimensional Turbulent Flow around a Bluff Body in Ground Proximity, AIAA Journal, vol. 27, no. 9.
4. Hucho, W., "Aerodynamics of Road Vehicles," Society of Automotive Engineers, Inc., Warrendale, Pa, 1998, ISBN 978-0-7680-0029-0.
5. Ahmed, S., Ramm, G., and Faltin, G., "Some Salient Features Of The Time-Averaged Ground Vehicle Wake," SAE Technical Paper 840300, 1984, doi:10.4271/840300.
6. Gilliéron, P. and Kourta, A., 2009. Aerodynamic drag reduction by vertical splitter plates, Experiments in Fluids, vol. 48, no. 1, 1-16.
7. Mair, W.A., "Drag-Reducing Techniques for Axi-Symmetric Bluff Bodies," in Aerodynamic Drag Mechanisms of Bluff odies and Road Vehicles," Plenum Press, New York, 1978, pp. 161-187.
8. Lanser, W., Ross, J., and Kaufman, A., "Aerodynamic Performance of a Drag Reduction Device on a Full-Scale Tractor/Trailer," SAE Technical Paper 912125, 1991, doi:10.4271/912125.
9. Mansingh, V., & Oosthuizen, P.H., "Effects of Splitter Plates on the Wake Flow Behind a Bluff Body", AIAA J., V. 28, pp.778-783, 1990.
10. Salari, K., Rutledge, W. and McBride, D. "Computational Prediction of Aerodynamic Drag for a Simplified Truck Geometry," U.S. DOE Third Workshop on Heavy Vehicle Aerodynamics, November 1999.
11. Nash, J.F., Quiency, V.G. & Callinan, J. "Experiments on Two-Dimensional Base Flow at Subsonic and Transonic Speeds," ARC R & M 3427.
12. Khalighi, B., Chen K-H and Iaccarino, G., "Unsteady Aerodynamic Flow Investigation around a Simplified Square-Back Road Vehicle with Drag Reduction Devices", J. Fluids Eng. 134(6), 061101 (May 29, 2012), doi:10.1115/1.4006643.
13. Al-Garni, A., Bernal, L., and Khalighi, B., "Experimental Investigation of the Near Wake of a Pick-up Truck," SAE Technical Paper 2003-01-0651, 2003, doi:10.4271/2003-01-0651.
14. Yang, Z. and Khalighi, B., "CFD Simulations for Flow Over Pickup Trucks," SAE Technical Paper 2005-01-0547, 2005, doi:10.4271/2005-01-0547.
15. Holloway, S., Leylek, J., York, W., and Khalighi, B., "Aerodynamics of a Pickup Truck: Combined CFD and Experimental Study," *SAE Int. J. Commer. Veh.* 2(1):88-100, 2009, doi:10.4271/2009-01-1167.
16. Fluent Version. 15.0, ANSYS Inc., 2013.

Contact Information

Kuo-Huey Chen
Kuo-Huey.Chen@gm.com
General Motors Global R&D

The Engineering Meetings Board has approved this paper for publication. It has successfully completed SAE's peer review process under the supervision of the session organizer. The process requires a minimum of three (3) reviews by industry experts.

ISSN 0148-7191

http://papers.sae.org/2015-01-1541